Contents lists available at ScienceDirect

Fundamental Research

journal homepage: http://www.keaipublishing.com/en/journals/fundamental-research/

Article

Using endogenous glycogen as relaxation agent for imaging liver metabolism by MRI

Shizhen Chen [a,b,c,1], Mou Jiang [a,b,1], Yaping Yuan [a,c], Baolong Wang [a,b], Yu Li [a], Lei Zhang [a,b,c], Zhong-Xing Jiang [a,c], Chaohui Ye [a,b,c], Xin Zhou [a,b,c,*]

[a] *State Key Laboratory of Magnetic Resonance and Atomic and Molecular Physics, National Center for Magnetic Resonance in Wuhan, Wuhan Institute of Physics and Mathematics, Innovation Academy for Precision Measurement Science and Technology, Chinese Academy of Sciences, Wuhan 430071, China*
[b] *Wuhan National Laboratory for Optoelectronics, Huazhong University of Science and Technology, Wuhan 430074, China*
[c] *University of Chinese Academy of Sciences, Beijing 100049, China*

ABSTRACT

Glycogen plays essential roles in glucose metabolism. Imaging glycogen in the liver, the major glycogen reservoir in the body, may shed new light on many metabolic disorders. ^{13}C magnetic resonance spectroscopy (MRS) has become the mainstream method for monitoring glycogen in the body. However, the equipment of special hardware to standard clinical magnetic resonance imaging (MRI) scanners limits its clinical applications. Herein, we utilized endogenous glycogen as a T_2-based relaxation contrast agent for imaging glycogen metabolism in the liver *in vivo*. The *in vitro* results demonstrated that the transverse relaxation rate of glycogen strongly correlates with the concentration, pH, and field strength. Based on the Swift-Connick theory, we characterized the exchange property of glycogen and measured the exchange rate of glycogen as 31,847 Hz at 37 °C. Besides, the viscosity and echo spacing showed no apparent effect on the transverse relaxation rate. This unique feature enables visualization of glycogen signaling *in vivo* through T_2-weighted MRI. Two hours-post intraperitoneal injection of glucagon, a clinical drug to promote glycogenolysis and gluconeogenesis, the signal intensity of the mice's liver increased by 1.8 times from the T_2-weighted imaging experiment due to the decomposition of glycogen. This study provides a convenient imaging strategy to non-invasively investigate glycogen metabolism in the liver, which may find clinical applications in metabolic diseases.

1. Introduction

Glycogen is a mixture of branched glucose polymers with α-1,4 and α-1,6 linkages between glucose units, found mainly in the liver and skeletal muscle but also partially in the brain, kidney, and intestine [1]. Glycogen is enormous and does not exist independently but binds to various proteins to form glycogen particles, which facilitates high water solubility. The formation of glycogen granules is closely related to hormone and enzyme levels in the body [2]. Theoretically, there is an intricate balance between glucose and glycogen concentrations in humans. However, abnormal glycogen metabolism will cause many metabolic diseases, like diabetes. Impairment of liver glucose regulation is an essential driving force in the early development of metabolic diseases such as diabetes mellitus type 2 (T2DM) [3]. Therefore, monitoring glycogen metabolism can be critical for disease diagnosis.

There are several non-invasive ways to detect glycogen, such as ^{1}H, ^{2}H, ^{13}C MRS [4–7], chemical exchange saturation transfer (CEST) MRI, and positron emission tomography (PET) [8]. ^{13}C-labeled glucose MRS has been one of the most used methods for *in vivo* glycogen detection over the past decades. Michael et al. used ^{13}C MRS to compare liver glycogen metabolism in type 2 diabetic patients and non-diabetic volunteers after mixed meals and successfully quantified postprandial net liver glycogen [9]. However, ^{13}C MRS measurement suffers from limited NMR sensitivity due to its low gyromagnetic ratio (^{13}C: 10.705 MHz T^{-1}, ^{1}H: 42.577 MHz T^{-1}) and low natural abundance (1.1% ^{13}C). Thus long acquisition time and large voxel size are necessary to achieve an adequate signal-to-noise ratio (SNR) in ^{13}C MRS. Besides, different radio frequency types of equipment, e.g., radiofrequency(RF) amplifier and coil at ^{13}C frequency, are required to perform ^{13}C MRS, which is rarely available on clinical MRI scanners. These factors significantly limit its clinical application in most hospitals. Likewise, ^{2}H MRS is restricted to its low NMR sensitivity and clinical accessibility. Besides, the resonance of glycogen overlaps inextricably with those of glucose in ^{2}H MRS [10,11]. PET with exogenous isotope labeling agent ^{18}F-NFTG is able to detect the synthesis of labeled glycogen, but the metabolic changes of total glycogen are unavailable in the liver.
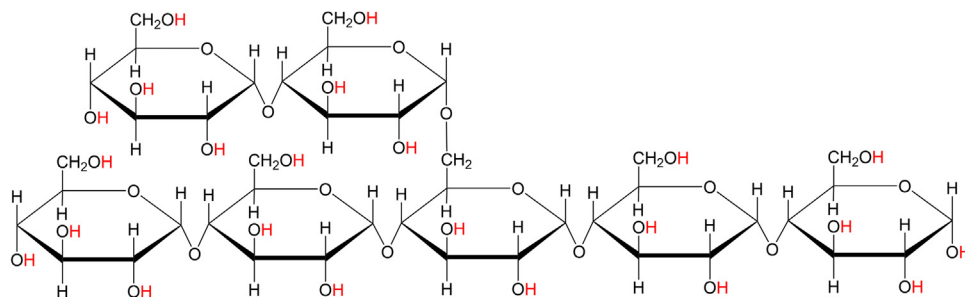
Fig. 1. Chemical structure of glycogen. Exchangeable protons, marked in red, are exchanged with water protons to produce T$_2$ contrast.

Glycogen Chemical Exchange Saturation Transfer (glycoCEST) is an emerging technique that indirectly detects glycogen through the exchange between glycogen hydroxyl protons and water protons [12,13]. It requires neither specialized hardware nor an exogenous contrast agent to provide a high-resolution glycogen map. Sherry et al. monitored liver glycogen metabolism after glucagon injection using glycoCEST [13]. However, due to the slight difference between the chemical shifts of glycogen exchangeable protons and water, glycoCEST is susceptible to the direct saturation effect of water, which affects its detection sensitivity. Several other endogenous molecules containing hydroxyl protons can have similar resonance frequencies that overlap with the glycogen exchangeable proton, which may hinder quantifying the intensity of glycoCEST [14]. Based on glycoCEST, glycogen nuclear Overhauser enhancement (glycoNOE) was developed as a novel method for detecting glycogen. Starting from the two NOE effect-based saturation transfer pathways from glycogen aliphatic protons to water, glycogen was indirectly detected by signal changes in water [15]. Using glycoNOE technology, Yadav et al. successfully monitored glycogen metabolism in the liver after fasting and glucagon injection with reasonable specificity [16]. Although CEST technology is an up-and-coming technology, CEST detection needs to collect a large amount of data and requires a long scanning time, which is a massive burden for the patients.

It has been reported that the presence of multiple labile protons in a single molecule, such as glucose, can be considered a transverse relaxation agent because they can carry out a rapid chemical exchange with water molecules, changing the transverse relaxation rate of water protons [17–19]. In this work, glycogen has been proven to be an effective endogenous T_2 relaxation contrast agent (Fig. 1). After intraperitoneal injection of glucagon to normal mice, the concentration of liver glycogen was reduced significantly, thus substantially affecting the transverse relaxation time of liver water. Through T_2-weighted MRI, we can monitor glycogen metabolic processes in the liver non-invasively and in real time.

2. Materials and methods

2.1. Materials

A 100 mM stock solution of bovine liver glycogen (Sigma) was prepared and then diluted to five different concentrations (0, 5, 10, 20, and 40 mM). Six samples at different pH values of 6.00, 6.50, 6.94, 7.34, 7.83, and 8.34 were obtained for each concentration. Each sample with 500 μL volume was poured into a cut-off 1 mL syringe, and imaging experiments were conducted on Bruker Biospec 4.7 T/30 cm and 9.4 T/30 cm MRI scanners at 20 °C. 1 mg porcine glucagon (Macklin) was dissolved in 1 mL saline for *in vivo* MRI experiments.

2.2. Methods

2.2.1. In vitro experiments

Quantitative T_2 measurements of all samples were performed using a manufacturer-supplied multi-slice multi-echo (MSME, Bruker) pulse sequence, and the same acquisition parameters were used on different MRI scanners. Three variable echo spacings were conducted with a total time of 3 s and the echo chain length/echo spacing were 200/15, 120/25, and 75/40, respectively. Other specific parameters are as follows: repetition time (TR) = 10,000 ms; number of averages = 1; matrix = 48 × 48; FOV = 4 cm^2; number of slices = 1; the slice thickness = 1 mm; and total scan time = 12 min. For quantitative T_1 measurements, a manufacturer-supplied fast spin-echo sequence (RARE, Bruker) was employed with the following parameters: TR value from 200 ms to 10,000 ms; echo time (TE) = 8 ms; RARE factor = 2; number of averages = 1; matrix= 48 × 48; FOV =4 cm^2; number of slices = 1; slice thickness = 1 mm; and the total scan time was 12.5 min. The T_2-weighted imaging was measured using an MSME pulse sequence on different MRI scanners with the following parameters: TR = 5 s; echo spacing = 20 ms; echo chain length = 80; number of slices = 1; slice thickness is 1 mm on 9.4 T scanner and 5 mm on 4.7 T scanner (to achieve a good SNR); matrix = 128 × 128; FOV = 4 cm^2; the total scan time was 6 min. Diffusion-weighted imaging (DWI) experiments were performed on each sample to confirm the effect of solution viscosity on relaxation time.

2.2.2. In vivo experiments

All experimental protocols involving animals were approved by the Animal Welfare and Research Ethics Committee at Innovation Academy for Precision Measurement Science and Technology, Chinese Academy of Sciences (Ethical number: APM21018T). For MRI experiments, healthy adult male C57BL/6 mice (n = 3) were anesthetized with 2%–3% isoflurane followed by 0.6–1 L/min flow of 1%–2% isoflurane to maintain anesthesia. Each mouse was intraperitoneally injected with 100 μL of glucagon solution (1.0 mg/mL) within 10 s and fixed to an animal bed in the prone position. Imaging experiments were performed immediately after the intraperitoneal injection of glucagon (within 4 min). T_2-weighted images of mice liver were acquired using RARE sequence with the following parameters: TR = 2 s; TE = 26 ms; RARE factor = 4; number of averages = 2; number of repetitions = 80; matrix size = 96 × 96; FOV = 30 mm × 25 mm; number of slices = 8 or 9; the slice thickness = 1 mm; and the total acquisition time was 128 min. Respiratory gating was applied during the scan to minimize the motion-related artifacts. Image processing was performed using a homemade MATLAB (MATLAB 2014b) script. All the T_2-weighted images were normalized to the first T_2-weighted image acquired within 4 min after intraperitoneal injection.

3. Results and discussion

3.1. In vitro experiments

The transverse relaxation rates (R_2) were measured for all the samples and the results showed a strong linear relationship between the concentration and R_2 (Fig. 2a). The results also indicated that the magnetic field strength positively correlated with R_2. To better explore the influence of the glycogen relaxivity (r_{2ex}), we fitted the data using Eq. 1:
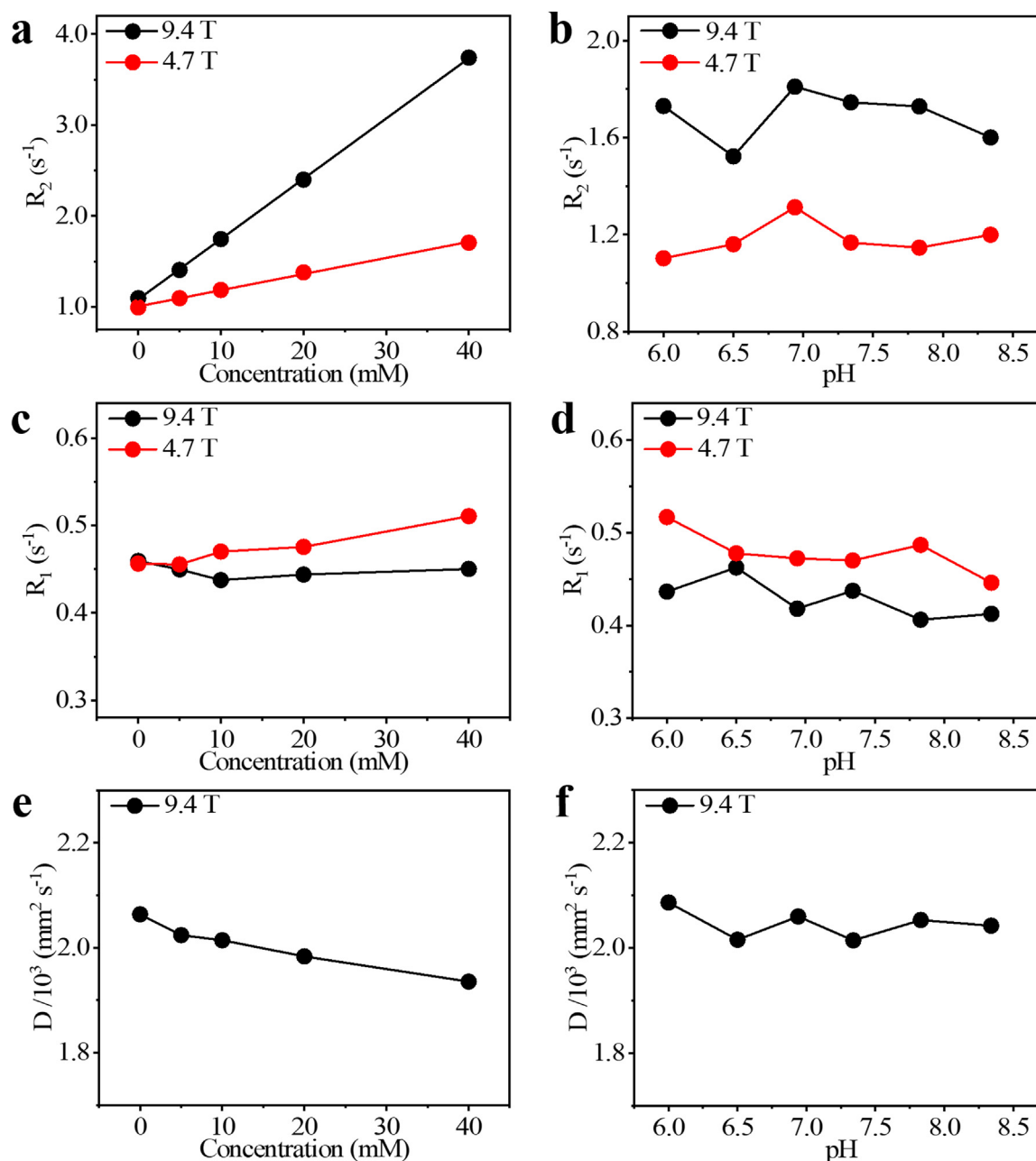
Fig. 2. Transverse relaxation rate, R_2 (a,b), longitudinal relaxation rate, R_1 (c,d), and translational diffusion coefficient, D (e,f) of glycogen solutions at 4.7 and 9.4 T measured at 20 °C. R_2 is linearly dependent on the concentration in the measured range, while pH is 7.34 (a), but the pH dependence of 10 mM glycogen is not (b). There is no apparent dependence between R_1 and concentration (c) or pH (d). D is independent of concentration (e) and pH (f).

$$R_2 = R_{2,\text{water}} + [\text{glycogen}]\, r_{2\text{ex,glycogen}} \qquad (1)$$

where we assumed that $r_{2\text{ex, glycogen}}$ can approximate the total relaxivity of glycogen. The $r_{2\text{ex, glycogen}}$ was 0.0663 s^{-1} mM^{-1} at 9.4 T under 20 °C, which is nearly 4 times larger than at 4.7 T (0.0178 s^{-1} mM^{-1}) (Fig. 2a).

The pH-dependent R_2 study showed that the R_2 of glycogen varied nonlinearly with pH, peaking at pH near 7 and then decreasing along both sides (Fig. 2b). The explanation for this phenomenon may be that glycogen is a branched polysaccharide, and the internal structure is dynamic equilibrium, thus exposing hydroxyl groups with different exchange rates at different pH values. Additional transverse relaxation experiments were performed on fresh rat blood to explore the influence of oxygen saturation (Table S1). The experimental results show that oxy-

gen saturation does not significantly affect glycogen's transverse relaxation rate under normal physiological conditions.

The viscosity is also an important factor that may affect the transverse relaxation rate of certain compounds, which can be reflected through the longitudinal relaxation rate (R_1) and diffusion coefficients (D) [20]. In order to explore this potential interference, the longitudinal relaxation rate and diffusion coefficients were measured on each sample. R_1 was not significantly correlated with glycogen concentration. The nonlinear variation of the longitudinal relaxation time may be affected by the ambient temperature fluctuation, the oxygen content in the solution, and the measurement error. At the same time, D decreased slightly (6%) with the increase in glycogen concentration (Fig. 2c and 2e). Therefore, the contribution of this slight variation to R_2 of glycogen could be ignored. There was no apparent relationship between R_1
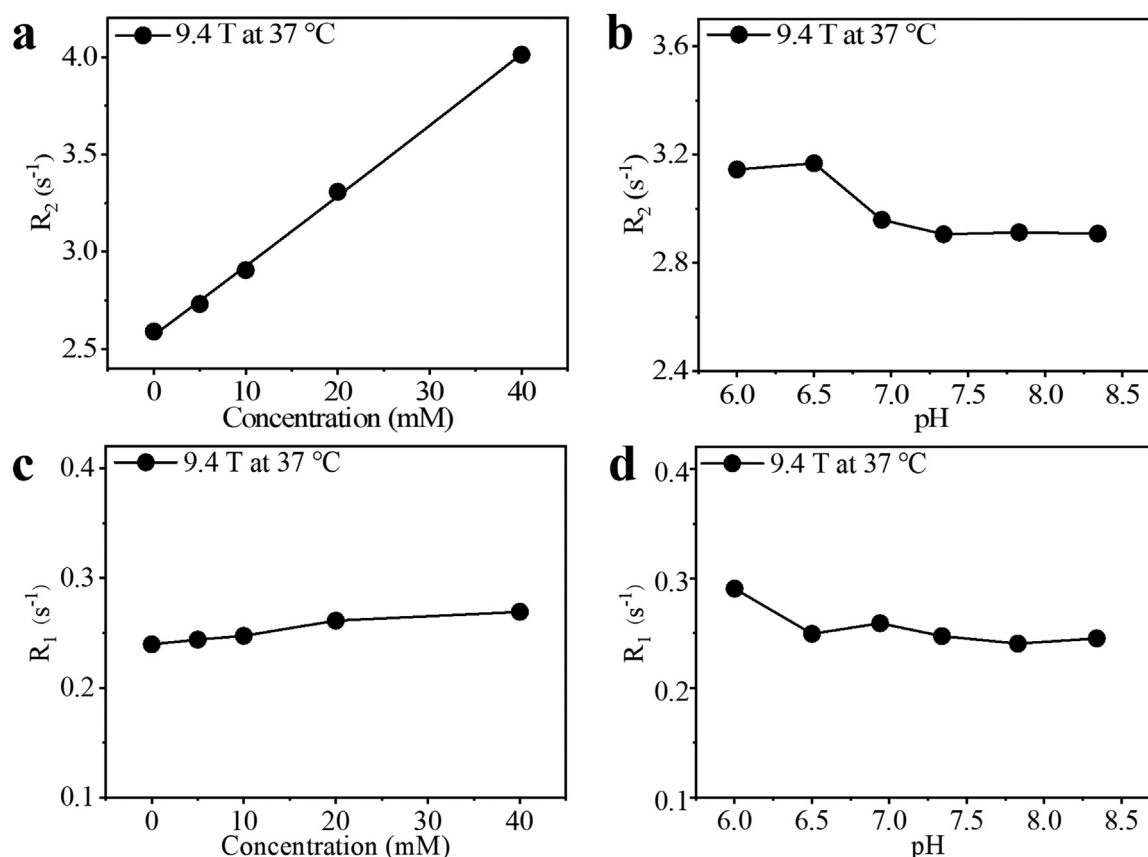
Fig. 3. Transverse relaxation rate, R_2 (a,b), longitudinal relaxation rate, R_1 (c,d) for glycogen solutions at 9.4 T measured at 37 °C. It has the same trend with the temperature at 20 °C.
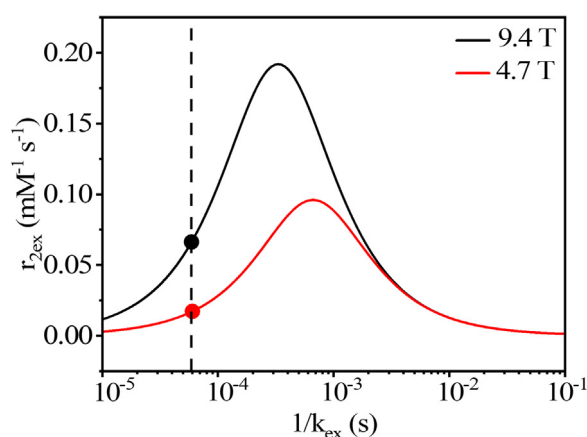
Fig. 4. Simulation of transverse relaxivity (r_{2ex}) at 4.7 and 9.4 T using the Swift-Connick equation. The markers are the measured experimental transverse relaxivity at each field under 20 °C. The fitted value is k_{ex}=16,667 s^{-1}.

or D and the pH of the glycogen solution within the measurement range (Fig. 2d and 2f). Therefore, the transverse relaxation rate of glycogen is mainly attributed to the exchange rate of the hydroxyl proton on glycogen, independent of solution viscosity [21]. To simulate the physiological environment, we also measured the relaxation time of each sample at 37 °C using the 9.4 T scanner. The results showed that the R_2 had a linear correlation with the concentration and no linear correlation with pH, and R_1 had no linear relationship with both the concentration and pH (Fig. 3).

To further investigate the exchange rate of glycogen, the Swift-Connick equation was used to analyze the transverse relaxivity [22]:

$$R_{2ex} = k_{ex} P_B \frac{R_{2B}^2 + R_{2B} k_{ex} + \Delta\omega^2}{\left(R_{2B} + k_{ex}\right)^2 + \Delta\omega^2} \qquad (2)$$

where R_{2B} is the transverse relaxation rate of exchangeable solute protons, and P_B is the mole fraction of exchangeable protons (for 1 mM glycogen, P_B = 14 mM exchangeable protons/110 M water protons). $\Delta\omega$ was set to 1.2 ppm in our case. Since $\Delta\omega \gg R_{2B}$, the transverse relaxivity (r_{2ex}) of glycogen can be approximated as

$$r_{2ex} = k_{ex} P_B \frac{\Delta\omega^2}{k_{ex}^2 + \Delta\omega^2}. \qquad (3)$$

In Fig. 4, we fitted the exchange rate correlation curves of exchangeable protons at 4.7 and 9.4 T, using Eq. 3. Combining the measured transverse relaxivity with the fitting curve, the exchange rate was calculated to be 16,667 s^{-1} (20 °C) and 31,847 s^{-1} (37 °C) at pH 7.34, which were falling into the left side of the Swift-Connick curves. With the temperature increase, the exchange rate becomes faster and r_{2ex} decreases, consisting of the transverse relaxivity behavior at 37 °C (Table 1). Although the glycogen consists of glucose, compared with glucose (2200 s^{-1}), glycogen has a higher exchange rate.

Based on the Swift-Connick equation, the r_{2ex} strongly depends on the chemical shift difference ($\Delta\omega$) between water and the exchangeable protons. For example, iron oxides (over 200 s^{-1} mM^{-1}) and paramagnetic T_{2ex} contrast agents (1–16 s^{-1} mM^{-1}) both exhibit high relaxivities [23]. Many diamagnetic molecules containing exchangeable protons show smaller chemical shift differences with water, leading to a slower exchange rate. Several diamagnetic T_2 contrast agents, such as D-glucose

Table 1
The transverse relaxivity and exchange rate of glycogen in different fields and at different temperatures.

Field (T)	$r_{2ex,\ glycogen}$ (s^{-1} mM^{-1})		k_{ex} (s^{-1})	
	20 °C	37 °C	20 °C	37 °C
4.7	0.0178	0.0090*	16,667	31,847
9.4	0.0663	0.0362		

* $r_{2ex,\ glycogen}$ at 37 °C was predicted based on exchange rate.

[19], D-maltose [17], and L-glutamine [18], have also been reported in the past decades. Comparatively, the glycogen has great advantages for imaging applications in the human body, especially the relatively large quantity compared to several other endogenous molecules.

Both T_{2ex} and CEST utilize the principle of chemical exchange. The difference is that CEST requires a relatively short or moderate exchange rate compared to the T_{2ex} mechanism. The ideal exchange rate for CEST imaging is 1–10 kHz. However, the exchange rate of exchangeable protons in glycogen solution is around 30 kHz at 37 °C, while pH is 7.34, which is too fast for CEST imaging. In addition, due to the different mechanisms of T_{2ex} and CEST, T_{2ex} is less affected by the magnetization transfer (MT) and nuclear overhauser effect (NOE). Since T_{2ex} does not require saturation frequency-dependent information, it requires less sampling time than CEST MRI. The T_{2ex} contrast focuses on the impact of the total exchangeable hydroxyl protons, while the CEST contrast focuses on specific saturation frequencies. According to different experimental needs, CEST and T_{2ex} images can provide two different complementary pieces of information.

Considering the spin-echo imaging method, the echo spacing can affect the transverse relaxivity. In an attempt to assess this influence, the transverse relaxivities at different echo spacings were measured (Fig. 5). Over the echo spacing tested from 15 to 40 ms, the transverse relaxivities were almost the same, demonstrating that the exchange rates of different hydroxyl protons on glycogen are very close. Compared to T_2-exchange behavior under different pHs and field strengths, the longitudinal relaxivities kept almost the same over the tested range.

Next, *in vitro* MRI experiments were performed with glycogen at field strengths of 4.7 and 9.4 T with different echo times using the MSME pulse sequence (Fig. 6). Considering the effect of SNR and the largest difference in the signal intensity in the decay curve, echo times were chosen with 160 and 600 ms for the experiments. The results showed that the T_2-weighted image of the glycogen has stronger contrast with the echo time increased. When the concentration increased, the intensity of the T_2-weighted image gradually weakened, with the signal intensity decreasing by 5.6% (ES = 160 ms) and 17.8% (ES = 600 ms) at 4.7 T using 20 mM glycogen solution and by 20.3% (ES = 160 ms) and 57.3% (ES = 600 ms) at 9.4 T.

3.2. In vivo experiments

We next turn our attention to an *in vivo* MRI study using glucogen as a T_2 exchange contrast agent. Glucagon is a clinical drug that promotes glycogenolysis and gluconeogenesis and thus significantly increases blood sugar concentration. The main target organ of the metabolic effect is the liver [24]. With the information in hand, we tentatively imaged the glycogen metabolism behavior in the liver with the help of glucagon. The T_2-weighted images were acquired 2 h after intraperitoneal infused with glucagon (100 μL, 1 mg/mL) in mice (Fig. 7). As shown in Fig. 7b, 15 min after intraperitoneal glucagon injection, the intensity of the liver began to increase and reached the maximum at 2 h. The enhancement of the liver T_2-weighted image intensity indicated that liver glycogen was decomposed into glucose as a drug effect of glucagon, and the transverse relaxation time of the liver water became longer.

In addition, it was also found that in the early stage of intraperitoneal injection of glucagon, the intensity of T_2-weighted imaging increased
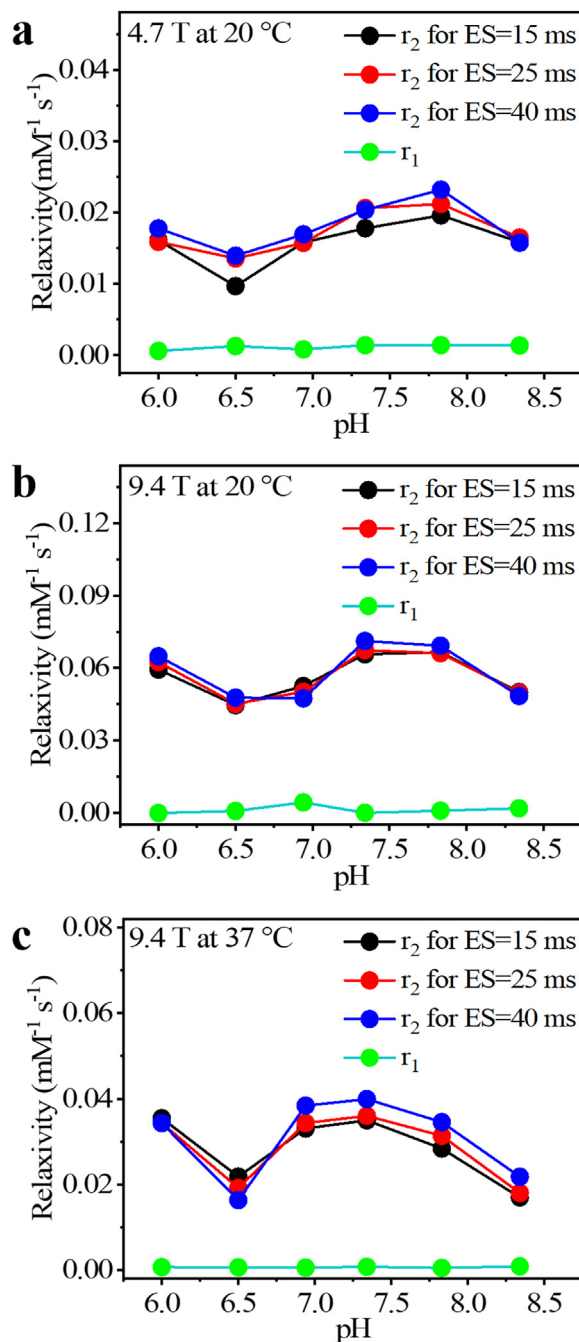
Fig. 5. Transverse and longitudinal relaxivity as a function of pH and echo spacing (ES) of 15, 25, and 40 ms at 4.7 T measured at 20 °C (a); 9.4 T measured at 20 °C (b); 9.4 T measured at 37 °C (c).

non-uniformly, and some of the local signals increased rapidly. After a while, the signal intensity tended to be uniform, consistent with the trend reported in the previous literature [10,16]. The observed changes in the spatial distribution of signal intensity following intraperitoneal injection may reflect the lobular anatomy of the liver, its vascularization and the heterogeneous distribution of glycogen in the liver [25]. Compared to the glucagon group, no significant change was observed in the signal intensity of the mouse liver after the infusion of saline (Fig. 7a). The results proved that most of the liver glycogen was in a relatively stable state and did not participate in metabolism. Through dynamic T_2-weighted liver imaging, we achieved real-time monitoring of hepatic glycogen metabolism in mice.
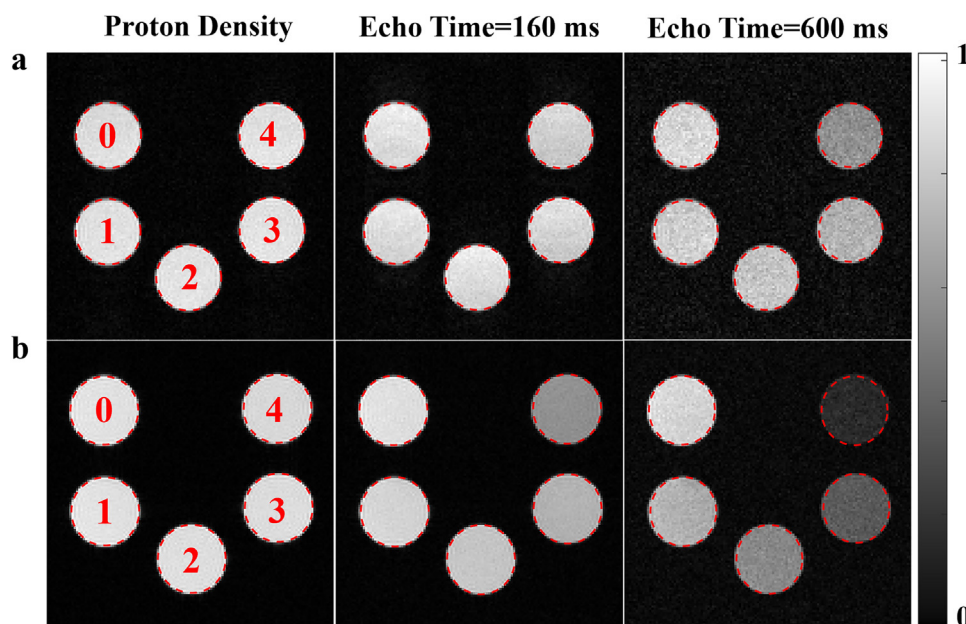
Fig. 6. T_2**-weighted images of glycogen solutions at 4.7 T (a) and 9.4 T (b) were measured at 20 °C.** In the left column are the proton density images, where 0, 1, 2, 3, and 4 represent glycogen concentrations of 0, 5, 10, 20, and 40 mM, respectively. The echo time of the middle column is 160 ms, and the right one is 600 ms.
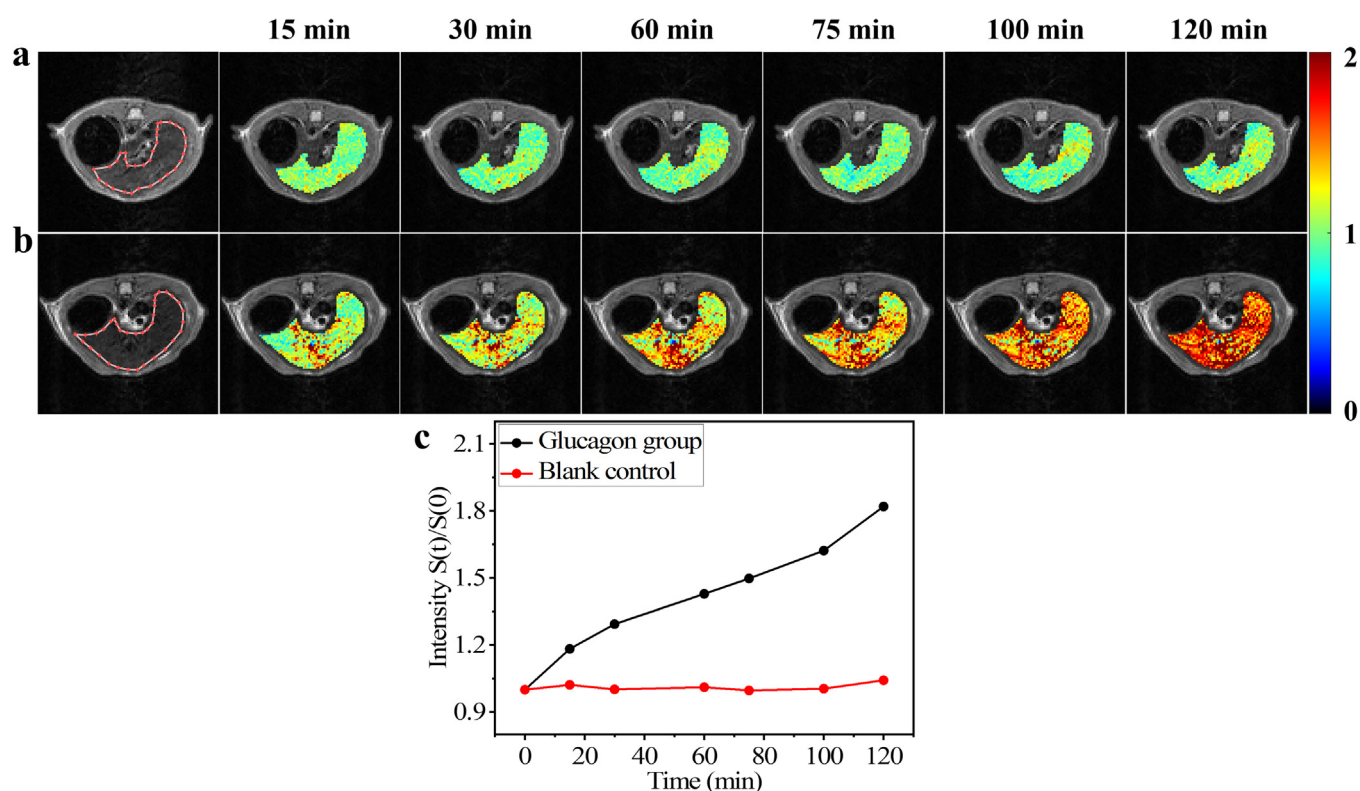
Fig. 7. Dynamic images of glycogen metabolism in the liver region of mice. Images were acquired with a T_2-weighted spin-echo sequence. (a) Infused with 100 μL of saline. (b) Infused with 100 μL of 1 mg/mL glucagon solution. (c) The intensity profiles of the liver region at different time points of each ROI.

4. Conclusion

In summary, we have successfully employed glycogen as an endogenous T_2 contrast agent to image liver glycogen metabolism. The transverse relaxation rate of glycogen is highly dependent on pH and magnetic field strength. When increasing the field strength to 9.4 T, the transverse relaxivity reaches 0.0362 mM^{-1}s^{-1} at 37 °C. The echo spac-

ing and viscosity show a neglectable effect on the transverse relaxation rate, which is beneficial for clinical glycogen imaging. *In vivo* results demonstrated that the T_2-weighted imaging signal intensity of the liver increased by 2 times after the injection of glucagon, attributed to the decomposing of glycogen in the liver. This work provides a new platform for non-invasively monitoring glycogen metabolism using MRI. Not only in normal mice, we hope the proposed method has the potential to be

applied to access abnormal glycogen metabolism-related liver diseases, such as obesity, hepatoma, diabetes type 2 (T2DM), and glycogen storage diseases.

Declaration of competing interest

The authors declare that they have no conflicts of interest in this work.

Acknowledgments

Supplementary materials

Supplementary material associated with this article can be found, in the online version, at doi:10.1016/j.fmre.2022.10.010.

References

[1] A.M. Brown, B.R. Ransom, Astrocyte glycogen and brain energy metabolism, Glia 55 (2007) 1263–1271.

[2] M.H.M. Rocha Leão, GLYCOGEN, in: B Caballero (Ed.), Encyclopedia of Food Sciences and Nutrition (Second Edition), Academic Press, Oxford, 2003, pp. 2930–2937.

[3] G.I. Shulman, D.L. Rothman, T. Jue, et al., Quantitation of muscle glycogen synthesis in normal subjects and subjects with non-insulin-dependent diabetes by 13C nuclear magnetic resonance spectroscopy, N. Engl. J. Med. 322 (1990) 223–228.

[4] R. Gruetter, I. Magnusson, D.L. Rothman, et al., Validation of 13C NMR measurements of liver glycogen in vivo, Magn. Reson. Med. 31 (1994) 583–588.

[5] T.B. Price, D.L. Rothman, M.J. Avison, et al., 13C-NMR measurements of muscle glycogen during low-intensity exercise, J. Appl. Physiol. 70 (1991) 1836–1844.

[6] R.B. van Heeswijk, F.D. Morgenthaler, L. Xin, et al., Quantification of brain glycogen concentration and turnover through localized 13C NMR of both the C1 and C6 resonances, NMR Biomed. 23 (2010) 270–276.

[7] L.H. Zang, D.L. Rothman, R.G. Shulman, 1H NMR visibility of mammalian glycogen in solution, Proc. Natl. Acad. Sci. USA 87 (1990) 1678–1680.

[8] T.H. Witney, L. Carroll, I.S. Alam, et al., A novel radiotracer to image glycogen metabolism in tumors by positron emission tomography, Cancer Res. 74 (2014) 1319–1328.

[9] M. Krssak, A. Brehm, E. Bernroider, et al., Alterations in postprandial hepatic glycogen metabolism in Type 2 diabetes, Diabetes 53 (2004) 3048–3056.

[10] H.M. De Feyter, M.A. Thomas, K.L. Behar, et al., NMR visibility of deuterium-labeled liver glycogen in vivo, Magn. Reson. Med. 86 (2021) 62–68.

[11] H.M.D. Feyter, K.L. Behar, Z.A. Corbin, et al., Deuterium metabolic imaging (DMI) for MRI-based 3D mapping of metabolism in vivo, Sci. Adv. 4 (2018) eaat7314.

[12] G.L. Simegn, A.J.W. Van der Kouwe, F.C. Robertson, et al., Real-time simultaneous shim and motion measurement and correction in glycoCEST MRI using double volumetric navigators (DvNavs), Magn. Reson. Med. 81 (2019) 2600–2613.

[13] P.C.M. v. Zijl, C.K. Jones, J. Ren, et al., MRI detection of glycogen in vivo by using chemical exchange saturation transfer imaging (glycoCEST), Proc. Natl. Acad. Sci. USA 104 (2007) 4359–4364.

[14] M. Deng, S.-Z. Chen, J. Yuan, et al., Chemical Exchange Saturation Transfer (CEST) MR technique for liver imaging at 3.0 Tesla: an evaluation of different offset number and an after-meal and over-night-fast comparison, Mol. Imaging Biol. 18 (2016) 274–282.

[15] P.C.M. van Zijl, N.N. Yadav, Chemical exchange saturation transfer (CEST): what is in a name and what isn't? Magn. Reson. Med. 65 (2011) 927–948.

[16] Y. Zhou, P.C.M. v. Zijl, X. Xu, et al., Magnetic resonance imaging of glycogen using its magnetic coupling with water, Proc. Natl. Acad. Sci. USA 117 (2020) 3144–3149.

[17] J.M. Goldenberg, M.D. Pagel, J. Cárdenas-Rodríguez, Characterization of D-maltose as a T2-exchange contrast agent for dynamic contrast-enhanced MRI, Magn. Reson. Med. 80 (2018) 1158–1164.

[18] C.G. Joo, S.-H. Yang, Y. Choi, et al., L-glutamine as a T2 exchange contrast agent, Magn. Reson. Med. 84 (2020) 2055–2062.

[19] N.N. Yadav, J. Xu, A. Bar-Shir, et al., Natural D-glucose as a biodegradable MRI relaxation agent, Magn. Reson. Med. 72 (2014) 823–828.

[20] M. Jamnongwong, K. Loubiere, N. Dietrich, et al., Experimental study of oxygen diffusion coefficients in clean water containing salt, glucose or surfactant: consequences on the liquid-side mass transfer coefficients, Chem. Eng. J. 165 (2010) 758–768.

[21] J. Jen, Chemical exchange and NMR-T2 relaxation, Adv. Mol. Relax. Process. 6 (1974) 171–183.

[22] T.J. Swift, R.E. Connick, NMR-relaxation mechanisms of O17 in aqueous solutions of paramagnetic cations and the lifetime of water molecules in the first coordination sphere, J. Chem. Phys. 37 (1962) 307–320.

[23] Z.-.T. Tsai, J.-.F. Wang, H.-.Y. Kuo, et al., In situ preparation of high relaxivity iron oxide nanoparticles by coating with chitosan: a potential MRI contrast agent useful for cell tracking, J. Magn. Magn. Mater. 322 (2010) 208–213.

[24] L. Rui, Energy metabolism in the liver, Comp. Physiol. 4 (2014) 177–197.

[25] B.F. Giffin, R.L. Drake, R.E. Morris, et al., Hepatic lobular patterns of phosphoenolpyruvate carboxykinase, glycogen synthase, and glycogen phosphorylase in fasted and fed rats, J. Histochem. Cytochem. 41 (1993) 1849–1862.

Shizhen Chen is a professor at Innovation Academy for Precision Measurement Science and Technology (APM), Chinese Academy of Sciences (CAS). Her research interests are focused on $^{129}Xe/^{19}F/^{1}H$ multi-nuclear magnetic resonance enhancement technology, and applications on early diagnosis of cancer.

Mou Jiang is currently a Ph.D. candidate under the supervision of Prof. Xin Zhou at Wuhan National Laboratory of Optoelectronics. His research interests focus on the application of endogenous magnetic resonance contrast agents.

Xin Zhou is the recipient of the "National Science Fund for Distinguished Young Scholars" and the "Youth Science and Technology Innovation Leader". He is the president of Innovation Academy for Precision Measurement Science and Technology (APM), Chinese Academy of Sciences (CAS). Xin Zhou has a long-term experience in the frontier research of magnetic resonance imaging (MRI) and spectroscopy focusing on ultrasensitive magnetic resonance imaging instruments, techniques, and biosensors for medical imaging.